Decoupling Genotype–Phenotype Resistance type in MDR *Klebsiella pneumoniae*: Integrative Genomic and Structural prudence into SULII, SULL and QnrB Determinants

Inas Sattar Abd
Department of Microbiology, College of Science, Al-karkh University of Science, Baghdad, IRAQ
Inasabd4@gmail.com

Abstract
Antimicrobial resistance in Klebsiella pneumoniae stays to trial therapeutic efficacy, predominantly when resistance genes contribute in complex cellular networks rather than acting as isolated determinants. This study investigates interplay between plasmid-mediated sulfonamide resistance genes (SULII, SULL) and quinolone resistance (QnrB) in multidrug-resistant (MDR) clinical isolates, with a focus on how sequence deviation translates or fails to translate into phenotypic resistance. Ten clinical isolates were described using a collective phenotypic–genotypic framework, comprising of antimicrobial susceptibility profiling, biofilm quantification, crystal violet assay and Sanger sequencing of SULII, SULL and QnrB. Molecular docking was employed to assess ciprofloxacin interface with the QnrB1 protein to further reveal structural contributions to resistance.

All isolates accommodated the three target genes and demonstrated either moderate or strong biofilm formation. Resistance phenotypes revealed no consistent association with minor allelic variations. Structural modeling discovered an optimal ciprofloxacin–QnrB1 binding energy of −6.08 kcal/mol, supporting a protecting rather than catalytic mechanism of resistance. Cooperatively, the findings emphasize that resistance in K. pneumoniae emerges from a multifactorial, network-dependent architecture rather than single-gene determinants. The study highpoints the limitations of conventional genotypic markers for prophesy clinical consequences and affirm the need to integrate whole-genome sequencing, transcriptomic data and structural biology to achieve resistance that is more accurate in forecasting and amended antibiotic surveillance.

Keywords: MDR, QnrB, SULII, SULL, Ciprofloxacin, VITEK 2.

Introduction

Klebsiella pneumoniae is a major opportunistic pathogen going to the family Enterobacteriaceae. Concerned in a wide range of hospital-acquired infections comprising of urinary tract infections, pneumonia and bloodstream infections, *K. pneumoniae* remains to represent a substantial universal health concern[16]. Above the past two decades, the clinical board of this organism has become progressively challenging, mainly due to its incredible ability to acquire and distribute antibiotic-resistance determinants[26]. The widespread genetic variability of *K. pneumoniae* donates directly to emergence of multidrug-resistant (MDR) strains, aided by its marked genetic plasticity and its ability to integrate antimicrobial resistance genes via horizontal gene transfer mechanisms, comprising of conjugation, transformation and transduction[28].

Between the most imperative resistance, determinants are plasmid-mediated quinolone resistance (PMQR) genes that subsidize to the evolution and transmission of resistance behaviors. These comprise of extended-spectrum beta-lactamases (ESBLs) and carbapenem-related genes for instance QnrB[1]. Subsequently, MDR strains show significant therapeutic obstacles, regularly resulting in continued hospital stays and augmented healthcare costs. In this circumstance, our investigation emphasizes on the distribution and features of SULI, SULII and QnrB genes in clinical *K. pneumoniae* isolates, in addition to the relationship between biofilm production and multidrug resistance.

Biofilm formation in *K. pneumoniae* improves the perseverance of bacterial communities on medical devices and donates to chronic infection by shielding cells from antimicrobial agents and host immune responses[11]. Biofilms are distinct as structured bacterial populations embedded indoors an extracellular polymeric substance (EPS) matrix composed of proteins, polysaccharides and nucleic acids[20].

This matrix suggestively decreases antimicrobial penetration, acting as a physical barrier and thus donating to frequent and persistent infections[33]. Remarkably, the ability of *K. pneumoniae* to form biofilms differs substantially between isolates, inducing both pathogenicity and clinical products[11].

The association among antimicrobial resistance and biofilm-forming capability in *K. pneumoniae* has been broadly studied[37]. In elevation, biofilm-producing isolates often reveal raised resistance levels, proposing a synergistic interaction among genetic resistance determinants and biofilm-mediated defensive mechanisms[36]. However,

outcomes in the literature stay unpredictable, underscoring the need for expanded investigations to elucidate this association in clinical isolates. Genes for instance SULI and SULII, related with sulfonamide resistance, have gained increasing attention predominantly in respiratory and urinary tract infections where these antimicrobials are recurrently employed[21]. In spite of this, the clinical influence of these genes between biofilm-producing strains residues underexplored. Phenotypic antibiotic susceptibility tests, PCR and Sanger sequencing are the molecular techniques usually used to investigate these characteristics.

This study provides serious perceptions that may augment current infection-control strategies by investigating the association between biofilm formation and genetic resistance profiles. Besides, it integrates detailed gene analyses aimed at describing mutations within resistance genes through genomic sequencing. These molecular modifications are crucial for clarifying the mechanisms essential resistance patterns, thus supporting accurate epidemiological surveillance and managing suitable therapeutic interventions.

Illustrating genetic variants in biofilm-producing strains also donates to establishing associations between heightened biofilm formation and specific resistance configurations, additionally revealing pathogen behavior in clinical settings. Eventually, the outcomes of this work may inform the development of developed therapeutic strategies and treatment strategies, donating to strengthened clinical practices, informed public-health interferences and the consideration of potential experimental treatment options.

Review of Literature

The phenomenon of antibiotic resistance in *Klebsiella pneumoniae* cannot be sufficiently understood as single genetic determinant; as a substitute, it must be approached as an integrated biological system in which multiple determinants interrelate dynamically. These determinants comprise of biofilm-forming ability, plasmid-encoded resistance loads, membrane and metabolic alteration and regulatory fluctuations in gene expression, all of that together shape the organism's adaptive site[12]. The present investigation is positioned within three major thematic directions steadily decorated in the literature. First, biofilm formation epitomizes a physiological and regulatory state that intensely modifies susceptibility patterns and permits the persistence of bacterial populations beneath antimicrobial pressure[3].

Second, plasmid-mediated determinants predominantly QnrB, a central constituent of the PMQR family significantly raise the basal resistance threshold to quinolones[29]. Third, the prevalent dissemination of sulfonamide-resistance genes SULII and SULL, beside their related mobile elements, remnants a defining feature of resistance to SXT and correlated compounds[17]. This study is an integrated methodological design integrating VITEK 2 automated susceptibility testing (aligned with CLSI guidelines), PCR, Sanger sequencing, quantitative crystal violet biofilm assays and molecular docking of ciprofloxacin with QnrB1 (PDB: 2XTY). This multi-layered methodology mirrors the dominant scientific consensus that antibiotic resistance establishes as an inherently complex and multi-factorial phenomenon[38].

Preceding work extensively agrees that biofilms function not only as passive physical barriers but also as regulatory middles that modify transcriptional programs encouraging efflux pump activation, decreasing porin expression and improving opportunities for horizontal gene transfer due to augmented cell density[5]. Empirical studies reliably prove that strong biofilm producers incline to exhibit broader resistance spectra, predominantly to late-generation cephalosporin and carbapenems[8]. Our outcomes follow this pattern: "strong" biofilm-forming isolates exhibited broader non-susceptibility profiles, comprising high resistance to ciprofloxacin and recurring resistance to SXT while tigecycline and colistin largely reserved effectiveness[10]. These notes reinforce the literature's importance on the interplay among membrane physiology and drug-resistance breadth.

A considerable body of evidence illustrates that Qnr proteins shield DNA gyrase and topoisomerase IV, rising the MIC baseline but infrequently generating high-level resistance except accompanied by QRDR mutations (e.g. gyrA, parC). Our sequencing consequences exposed widespread carriage of QnrB, nevertheless the minor positional variations detected did not correspond directly to alterations in CIP-R/CIP-S patterns.

Stable with structural reports, our docking analysis produced a binding energy of −6.08 kcal/mol, with ciprofloxacin positioned within a shallow QnrB1 surface groove forming primarily polar and hydrophobic interactions. Such a geometry consensus with the concept that Qnr proteins mediate surface protection slightly than direct catalytic interference[25]. Likewise, global epidemiological studies have recognized the spreading of sul genes through plasmids and integrons[24]. Nevertheless, our dataset discovered that small sequence variants within SULII/SULL did not relate dependably with SXT susceptibility, signifying that gene context (promoter activity, copy number, adjacency to dfrA) and subsidiary mechanisms for instance efflux and permeability play considerable roles[30].

Our isolates showed greatly conserved SULII/SULL sequences and the few substitutions existing concerning the primacy of genomic context over micro-polymorphism[13]. These tendencies further highpoint the need to incorporate functional metrics of efflux and permeability chiefly under biofilm conditions into explanatory models[15,31].

The literature states that vigorous inference necessitates the integration of multiple evidence layers:

1. Standardized AST according to CLSI/EUCAST guidelines[7].
2. PCR-based gene revealing coupled with sequencing to determination variant architecture[23].
3. The use of quantitative biofilm assays in place of qualitative markers[35].
4. A mechanistic interpretation layer is incorporated into structural-computational analysis.

At this point, the integrated architecture was implemented in the investigation: Numerous beta-lactams, carbapenems, aminoglycosides, fluoroquinolones, colistin, tigecycline and SXT have been employed in conjunction with VITEK 2. Sanger sequencing, crystal violet assay in 96-well plates and blind and directed molecular docking on QnrB1 were all performed subsequent to the PCR. The convergence of the models was enhanced and the reliability of inferring the structural orientation of the interaction with ciprofloxacin increased via this process. The literature recommendations are not only matched by this combination, but they also offer a more precise interpretation of the discrepancies between genotype and phenotype.

A growing body of literature has confirmed that the severity of biofilms is correlated with the extent of resistance. This is due to the fact that cells in this structure assume a distinct metabolic-regulatory pattern, in addition to their function as a "permeability barrier". In our data, we observed a distinct visual correlation between the breadth of drug resistance and high membrane severity. This confirms the notion that the prevalence of MDR in the general population is due to the high biofilm capacity. The absence of a direct correlation between the ciprofloxacin phenotype and the micro-polymorphism of the QnrB gene in all isolates, as well as our detection of the gene on the PMQR side, is directly consistent with existing reports.

The reports support the idea that Qnr protein protection needs to combine with QRDR mutations and hypersecretion to produce clinically significant resistance. On the SXT side, the high sequence conservation of SULII/SULL, coupled with the absence of a definitive match to the phenomenon, places the "gene context" (transcript/promoter/integron/ sul/dfrA kit) at the heart of the causal explanation. These overlaps with the general trend give our results greater reliability and demonstrate the validity of our choice of these markers.

Recent review conclusions agree that gene presence alone is not sufficient for phenotypic prediction and that its dosage (plasmid copy number/promoter strength), location (on a host integrin/broad-spectrum plasmid), expression (transcriptional irradiation conditions) and proximity (e.g. with dfrA/sul1/sul3) determine clinical outcome. Our results support the following view: Minor SULII/SULL sequence variations alone did not explain SXT resistance and the equal burden of QnrB substitutions across three isolates did not preclude differences in CIP and MDR status. Therefore, in line with lessons learned, we believe that confirming the causative factors requires complementary tools. These tools include: qPCR (for copy number), whole-genome sequencing (WGS) (to determine gene load and insertion sites) and transcriptomic analyses (to measure expression in biofilm conditions). We explicitly indicated in our discussion that these subsequent tests will help to resolve the genetic basis of SXT resistance and clarify the roles of QRDR/excretion in quinolone resistance. To understand how Qnr proteins interact with fluoroquinolones, numerous structural studies based on molecular docking and simulations were conducted.

While these studies often show intermediate binding energies and shallow positions, we revealed through a blind and then guided protocol that narrowing the search box to the candidate groove on QnrB1 increased the conformational preference and increased the conformational convergence.

This yielded an optimal energy of 6.08 kcal/mol and geometric consistency, suggesting a shallow, polar network of interactions that supports cross-protection over direct inactivation. Our interpretation of the relationship between QnrB prevalence and CIP patterns in our isolates is enhanced by this mechanistic dimension. In the absence of a one-to-one correlation at the sequence level, it serves as an explanatory bridge between gene and phenomenon, as suggested by the literature. In light of the above, it can be seen that this work contributes as embodied in three interconnected points:

1. An experimental bridge between genotype and phenotype showing that the presence of QnrB/SULII/SULL is common among isolates. It also reveals that biofilm strength is associated with the breadth of multi-chain resistance in a clinical sample.
2. A regulatory-dose argument against reducing interpretation to a "minor polymorphism" in the gene with subsequent measurable pathways (copy number/expression/integron/dfrA) being presented as the keys.
3. A structural attribution that explains the mechanism of QnrB1 in target protection and partially explains the common insensitivity to ciprofloxacin.

Accordingly, this study has provided a case study that reframes the "big picture" of the literature and confirms that a "layers of evidence" approach from AST to structural genomics is the most robust path to understand MDR in *K. pneumoniae*.

Methods

Isolation and identification of Bacterial: Clinical isolates of *K. pneumoniae* were attained from a spectrum of diagnostic specimens, comprising of sputum, urine, wound swabs and blood cultures collected from hospitalized patients. Initial phenotypic identification was conducted using the VITEK 2 Compact automated system

(BioMérieux, France), following standard operating procedures. All isolates were then preserved in Brain Heart Infusion broth supplemented with 20% glycerol and stored at –80 °C to conserve genetic and phenotypic immovability for downstream analyses.

Antimicrobial Susceptibility Testing (AST): Antimicrobial susceptibility profiling was done using the VITEK 2 compact system, using the panel suggested by the manufacturer. The antimicrobial agents tested comprised: ampicillin/sulbactam, cefotaxime, piperacillin/tazobactam, ceftazidime, ceftolozane/tazobactam, ceftazidime/ avibactam, imipenem, cefepime, meropenem, amikacin, ciprofloxacin, colistin, tigecycline and trimethoprim/ sulfamethoxazole. Interpretation of minimum inhibitory concentration (MIC) consequences adhered strictly to CLSI performance standards. Multidrug resistance was distinct as non-susceptibility to ≥3 antimicrobial classes.

Extraction of DNA and PCR Amplification: Genomic DNA was extracted by means of the G-spin™ DNA Extraction Kit (Intron Biotechnology, Korea), applying the manufacturers optimized protocol. Concisely, overnight cultures were centrifuged to achieve bacterial pellets followed by enzymatic lysis with Proteinase K at 56°C for 30 min. The lysates endured subsequent binding, washing and elution steps to harvest purified DNA. DNA concentration and purity (A260/A280) were measured using a Nanodrop™ spectrophotometer.

PCR evaluations were conducted to identify resistance genes, comprising QnrB, SULII and SULL. PCR reactions were prepared using Maxime PCR PreMix kits (i-Taq, Intron Biotechnology, Korea), with specific primers synthesized by Integrated DNA Technologies (USA). The primer sequences were as follows: QnrB (forward: 5'-GGMATHGAA ATTCGCCACTG-3', reverse: 5'-TTTCGCGGCGTTGC TGGG-3'), SULII (forward: 5'-TCCGGTGGAGGCCGGT ATCTGG-3', reverse: 5'-CGGGAATGCCATCTGCCTTG AG-3') and SULL (forward: 5'-TTCGGCATTCTGAATCT CAC-3', reverse: 5'-ATGATCTAACCCTCGGTCTC-3').

Thermal cycling conditions involved initial denaturation at 94°C for five min. followed by 30 cycles. Each cycle consisted of denaturation at 94°C for 30 seconds followed by annealing at an optimized temperature for 30 seconds for each primer. The cycle ended with a 60-second extension at 72°C followed by a final extension step at 72°C for 7 minutes. PCR products were investigated by electrophoresis on 1.5% agarose gels stained with Red safe nucleic acid staining solution (Korea, Intron Biotechnology) and visualized under UV illumination using Vilber Lourmat imaging system (France).

Sequencing and Analysis: The PCR amplicons were purified by a viable purification kit (Intron Biotechnology, Korea) and subjected to bidirectional Sanger sequencing to confirm high-fidelity sequence determination. Sequence chromatograms were curated and edited using BioEdit software. Identity approval and comparative analyses were achieved using BLASTn searches against the NCBI GenBank database. Multiple sequence alignment and variant analysis were directed to detect probable polymorphisms or mutation signatures related with antimicrobial resistance.

Biofilm Formation Assay: Biofilm-forming capability was assessed using the standardized crystal violet microtiter plate assay. Overnight cultures were used to 0.5 McFarland in sterile saline, after that 180 µl of BHI + 1% glucose was dispensed into separate well of sterile 96-well polystyrene plates, followed by inoculation with 20 µl of bacterial suspension. Plates were incubated at 37°C for 24 h below static aerobic conditions. Post-incubation wells were softly washed thrice with phosphate-buffered saline to eradicate planktonic cells. Biofilms were fixed with 150 µl methanol for 15 min and stained with 1% crystal violet for 15 min. Additional dye was eliminated by thorough washing with D.W and the plates were dried at 37°C. Bound dye was solubilized using ethanol (95%) and absorbance was measured by using microplate reader at 595nm. Isolates were considered into non-producers, strong moderate or weak, biofilm producers based on recognized absorbance cutoffs.

Preparation for protein: The crystal structure of QnrB1 (PDB ID: 2XTY, 2.8 Å resolution) was recovered from the RCSB Protein Data Bank. Structural preprocessing was achieved using PyMOL v3.1.1 (Schrödinger, LLC), comprising the exclusion of water molecules, heteroatoms and non-essential ligands, followed by adding all missing hydrogen atoms. Protonation situations dispersed at physiological pH by means of AutoDockTools (ADT) v1.5.7. Energy minimization was afterwards accompanied using the GROMOS96 force field through the Swiss sidechain minimization server, confirming optimal stereo chemical geometry and exclusion of steric clashes prior to computational analyses.

Ligand preparation: The 3D structure of ciprofloxacin (PubChem CID: 2764) was downloaded from the PubChem database in SDF format. The ligand was converted to PDB format and protonated at physiological pH. ADT assigned Gasteiger charges and defined torsional degrees of freedom. They then saved the ligand in PDBQT format for docking.

Blind docking: Initial blind docking with Auto Dock Vina (version 1.2.5) explored the entire protein surface for potential binding sites. Then, we set the grid box dimensions to encompass the entire protein, with center coordinates derived from the protein centroid. Exhaustion was set to 32 to ensure sufficient conformational sampling. Finally, the output poses were ranked according to Vina's scoring function (binding free energy, kcal/mol).

Focused docking: We performed a focused docking run after identifying the highest-probability binding region in the

blind docking. The grid box was centered at the coordinates of the best-scoring blind docking pose (X = –26.406, Y = 16.461, Z = –33.993) with dimensions of 20 × 20 × 20 Å to cover the binding pocket and nearby loops. The same docking parameters were applied.

Visualization and interaction analysis: We visualized the docking results in PyMOL. Protein loops implicated in fluoroquinolone resistance (Loop A: residues 46–53; Loop B: residues 102–113) were highlighted and PRP faces were color-coded. Ligand–protein hydrogen bonds, π–π interactions and hydrophobic contacts were identified using BIOVIA Discovery Studio Visualizer (version 2021). Figures were rendered at 300 dpi for publication.

Statistical Analysis: Python (version 3.11) was used to complete statistical analyses. Specifically, we employed pandas, scipy and numpy libraries for data management and statistical testing. The association between biofilm formation intensity and MDR phenotype was evaluated using Fisher's exact test due to limited sample size. A P-value of less than 0.05 was statistically significant. Data were accessible in contingency tables and results were interpreted considering clinical and epidemiological significance.

Results

As shown in figure 1, across panels A–C, all samples yielded single, sharp bands that co-migrate with the expected sizes (433, 293 and 469 bp respectively). This indicates specific amplification without detectable non-specific products or primer–dimers. Band intensities are broadly comparable between lanes, supporting consistent DNA input and amplification efficiency. The absence of additional bands and smearing suggests good DNA integrity and adequate PCR optimization (primer design, Mg^{2+}, annealing temperature). Collectively, these gels confirm that the target loci were successfully and specifically amplified and are suitable for downstream analyses (e.g. Sanger sequencing or restriction analysis).

The 96-well crystal-violet assay quantified biofilm production, showing that all 10 isolates were biofilm producers. The distribution skewed toward higher intensities: 6 out of 10 (60%) isolates being moderate producers and 4 out of 10 (40%) being strong producers. No weak or non-producers were detected (Figure 2).

Across the ten isolates, resistance clustered with biofilm strength (Figure 3). Isolates with strong biofilm tended to show broad resistance spanning third-/fourth-generation cephalosporins, β-lactam/β-lactamase–inhibitor combinations and carbapenems (imipenem, meropenem). The resistance also frequently included aminoglycosides. In contrast, most moderate biofilm isolates remained susceptible to carbapenems and aminoglycosides and exhibited a narrower resistance profile. Ciprofloxacin resistance was common (with a single intermediate case) and trimethoprim/sulfamethoxazole resistance was frequent. Tigecycline and colistin retained activity against the majority of isolates.

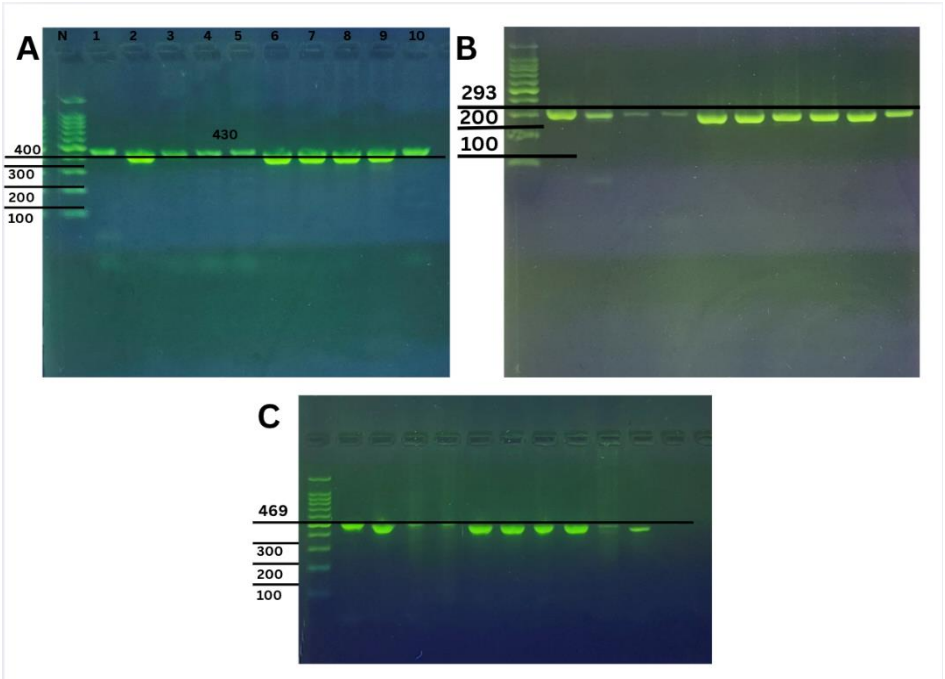

Figure 1: Representative gels showing single amplicons at the expected sizes. (A) Lanes 1–10: 433-bp product; N: 100-bp DNA ladder. Run on 2% agarose in 1×TBE at 7.5 V/cm (≈75 V across a 10-cm gel) for 60 min. (B) Lanes 1–10: 293-bp product; N: 100-bp DNA ladder. Run on 2% agarose in 1×TBE at 7.5 V/cm for 60 min. (C) Lanes 1–10: 469-bp product; N: 100-bp DNA ladder. Run on 1.5% agarose in 1×TBE at 5 V/cm for 60 min. Guidelines at 100, 200, 300 bp (and at the target band in each panel) are shown for orientation.

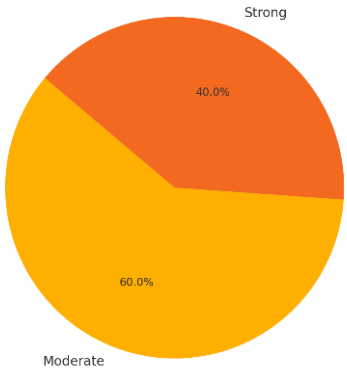

Figure 2: Pie Chart of Biofilm Strength Distribution.

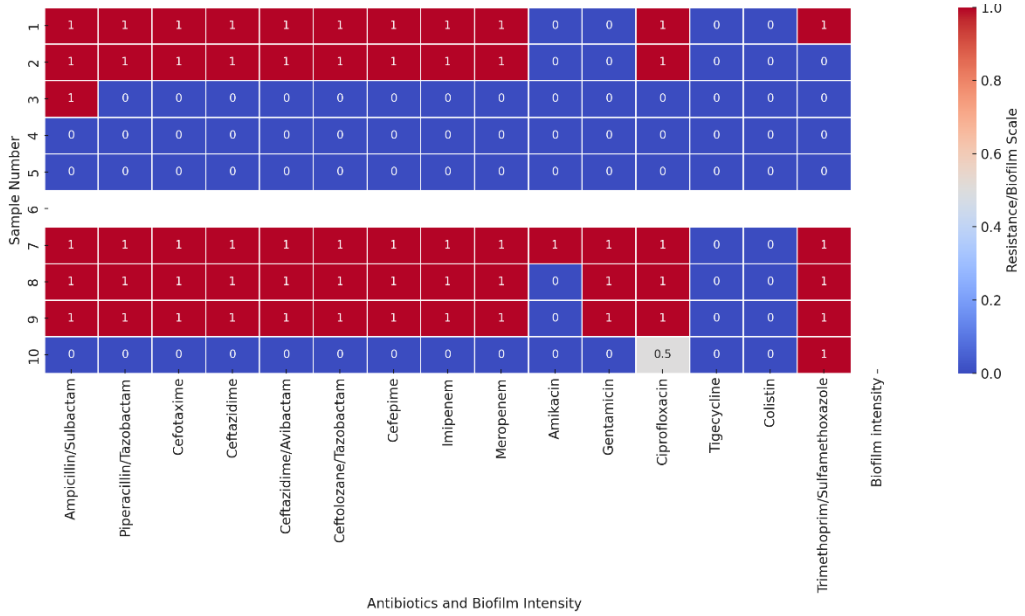

Figure 3: This heatmap illustrates the antibiotic resistance profiles isolated from *K. pneumoniae* in relation to the intensity of biofilm production. Each row represents an isolate and each column corresponds to a specific antibiotic or the biofilm intensity score. The codes of resistance values are as follows: 1 for resistant (R), 0.5 for intermediate (I) and 0 for sensitive (S). Biofilm intensity is numerically scaled as 0 (none), 1 (weak), 2 (moderate) and 3 (strong). The color gradient highlights potential associations between multidrug resistance and biofilm-forming capability across the clinical isolates.

All study amplicons matched known QnrB alleles with high nucleotide identity (97–98%) and no large indels, confirming correct target amplification. The observed variation consisted of scattered single-base substitutions, a mix of transitions (e.g. C→T, G→A) and transversions (e.g. C↔A, C↔G, T↔A)—plus a few single-nucleotide gaps. As illustrated in figure 4, this pattern is consistent with the natural allelic diversity reported among QnrB variants (e.g. QnrB12/QnrB60). Table 1 summarizes the gene QnrB sequence alignment results.

Test 1: *Klebsiella pneumoniae* DNA, contains quinolone-resistant protein-like sequence, clone: qnrB60. Sequence ID: AB894352.1 Length: 449 Number of Matches: 1. Range 1: 17 to 446 GenBank Graphics Next Match Previous Match. The alignment statistics that we used in match#1 are as follows:

Score: 743 bits (402), Expect (0.0), Identities: 425/435 (98%), Gaps: 6/435 (1%) and Strand (plus/plus)

Across the isolates, the substitution count in qnrB (all = 8) did not map one-to-one onto ciprofloxacin phenotype or MDR status: isolate 2 was CIP-R, isolate 1 was CIP-S and MDR status varied despite identical qnrB variation. As listed in table 2, all three showed moderate biofilm. The SULII targets were highly conserved (≈99% identity) across isolates (Table 3). The only variation is limited to isolated transversions and single-base gaps, with no evidence of large indels within the amplified region. The strongest match to a plasmid locus (CP153458.1) supports a mobile-element context for SULII in these isolates.

Test 2: *Klebsiella pneumoniae* strain NK_H2_020 plasmid pNK_H2_020.1, complete sequence is shown in figure 5.

Sequence ID: CP153458.1 Length: 257786 Number of Matches: 1. Range 1: 31029 to 31267 GenBank Graphics Next Match Previous Match. The alignment statistics that we used in match#1 are as follows:

Score: 435 bits (235), Expect (2-117), Identities: 238/239 (99%), Gaps: 1/239 (0%) and Strand (plus/plus).

In the isolates, small differences in SULII polymorphism (1–2 substitutions) did not track directly with SXT phenotype or overall MDR status. For example, the isolate with one substitution was SXT-resistant and MDR whereas isolate 2, which had two substitutions, was SXT-susceptible and non-MDR, all with moderate biofilm (Table 4). These include the presence of other sul genes (e.g. sul1/sul3), trimethoprim resistance determinants (dfrA variants), integron/promoter context, or broader mechanisms (efflux/porin changes). Follow-up tests, such as qPCR for copy number, targeted PCR for sul1/sul3/dfrA, or WGS, would help to resolve the genetic basis of SXT resistance in this set.

Based on table 5, SULL was highly conserved across the sequenced isolates (identities 98.75–99.25%). The variation was limited to a few transversions and single-nucleotide gaps; no large indels were detected within the amplified region. The top matches to plasmid sequences (e.g. CP110179.1) support carriage on mobile elements, consistent with dissemination of sulfonamide resistance in *K. pneumoniae*. These include gene context/expression, copy number, presence of other sul or dfr genes, or broader permeability/efflux effects.

Test 3: *Klebsiella pneumoniae* strain XYJ-CZA-R plasmid pXYJ-CZA-R-2, complete sequence (Figure 6). Sequence ID: CP110179.1 Length: 95599 Number of Matches: 1. Range 1: 93479 to 93883 GenBank Graphics Next Match Previous Match. The alignment statistics that we used in match#1 are as follows:

Score: 719 bits (389), Expect (0.0), Identities: 400/405 (99%), Gaps: 2/405 (0%) and Strand (plus/plus).

The results in table 6 show the isolate with the highest SULL variation (5 substitutions), which is SXT-resistant with MDR. Isolates 2–3 carry fewer substitutions (2–3) and are SXT-susceptible and non-MDR. All of them are also moderate biofilm producers. These include gene context and dosage (copy number/promoter strength) and the presence of other determinants (e.g. sul1/sul2/sul3 and dfrA variants for trimethoprim resistance) as well as efflux/porin effects.

Blind docking yielded modest scores (best –5.17 kcal/mol) distributed across multiple surface locations. Constraining the search around the candidate groove improved the ranking, with a best focused pose of –6.08 kcal/mol (mode 1; RMSD = 0 Å).

```
Query  12   CGATGCTGACGATGCCATTTTTAAAAGCATGTACATTTATCCATGGCGCGGTTTTTCGCA  71
            ||||||||| |||||||||||||||| |||  |||||||||  | |||| |||||||
Sbjct  17   CGATGCTGAAGATGCCATTTTTAAAAGC-TGT-GATTTATCCAT-G-GCGGATTTTCGCA  72
Query  72   ATTCCAGTGCGCTGGGCATTGAAATTCGCCACTGCCGCGCACAAGGCGCAGATTTCCGCG  131
            ||||||||||||||||||||||||||||||||||||||||||||||||||||||||||||
Sbjct  73   ATTCCAGTGCGCTGGGCATTGAAATTCGCCACTGCCGCGCACAAGGCGCAGATTTCCGCG  132
Query  132  GCGC-AGCTTTATGAATATGATCACCACGCGCACCTGGTTTTGTAGCGCATATATCACGA  190
            |||| ||||||||||||||||||||||||||||||||||||||||||||||||||||||
Sbjct  133  GCGCAAGCTTTATGAATATGATCACCACGCGCACCTGGTTTTGTAGCGCATATATCACGA  192
Query  191  ATACCAATCTAAGCTACGCCAATTTTTCGAAAGTCGTGTTGGAAAAGTGTGAGCTGTGGG  250
            ||||||||||||||||||||||||||||||||||||||||||||||||||||||||||||
Sbjct  193  ATACCAATCTAAGCTACGCCAATTTTTCGAAAGTCGTGTTGGAAAAGTGTGAGCTGTGGG  252
Query  251  AAAACCGTTGGATAGGTGCCCAGGTACTGGGCGCGACGTTCAGTGGTTCAGATCTCTCCG  310
            ||||||||||||||||||||||||||||||||||||||||||||||||||||||||||||
Sbjct  253  AAAACCGTTGGATAGGTGCCCAGGTACTGGGCGCGACGTTCAGTGGTTCAGATCTCTCCG  312
Query  311  GCGGCGAGTTTTCGACTTTCGACTGGCGAGCAGCAAACTTCACACATTGCGATCTGACCA  370
            ||||||||||||||||||||||||||||||||||||||||||||||||||||||||||||
Sbjct  313  GCGGCGAGTTTTCGACTTTCGACTGGCGAGCAGCAAACTTCACACATTGCGATCTGACCA  372
Query  371  ATTCGGAGTTGGGTGACTTAGATATTCGGGGCGTTGATTTACAAGGCGTTAAGTTGGACA  430
            ||||||||||||||||||||||||||||||||||||||||||||||||||||||||||||
Sbjct  373  ATTCGGAGTTGGGTGACTTAGATATTCGGGGCGTTGATTTACAAGGCGTTAAGTTGGACA  432
Query  431  ACTACAGGGGCATCG  445
            ||||| ||| |||||
Sbjct  433  ACTACCGGG-CATCG  446
```

Figure 4: Sequence alignment of the study QnrB amplicon to a reference allele (AB894352.1, *Klebsiella pneumoniae* clone QnrB60).

Table 1
Summary of the gene QnrB sequence alignment results.

***Klebsiella pneumoniae* qnrB**						
S.N.	**Type of substitution**	**Location**	**Nucleotide**	**Sequence ID with compare**	**Source**	**Identities**
1	GAP TRANSVERSION GAP TRANSVERSION TRANSITION GAP TRANSITION TRANSITION	30 31 43 48 68 119 261 362	A/- C/G C/- T/A G/A -/A C/T G/A	KP184842.1	*Klebsiella pneumoniae* strain K19-A2 quinolone resistance protein B12 (QnrB12) gene, partial cds	**98%**
2	TRANSVERSION GAP GAP TRANSVERSION GAP GAP TRANSVERSION GAP TRANSVERSION GAP	26 45 49 50 61 63 68 137 438 442	C/A A/- A/- C/G G/- C/- T/A -/A A/C G/-	AB894352.1	*Klebsiella pneumoniae* DNA contains quinolone-resistant protein-like sequence, clone: QnrB60	**98%**
3	TRANSVERSION GAP TRANSITION GAP TRANSVERSION GAP TRANSVERSION GAP GAP TRANSVERSION TRANSVERSION	26 40 41 48 49 61 66 136 435 437 438	C/A -/A G/A A/- C/G C/- T/A -/A C/- A/C G/C	AB894352.1	*Klebsiella pneumoniae* DNA contains quinolone-resistant protein-like sequence, clone: QnrB60	**97%**

```
Query  1      GCGACGC-AGCCTATGCCTTGTCGCGTGGTGTGGCCTATCTCAATGATATTCGCGGTTTT  59
              ||||||| ||||||||||||||||||||||||||||||||||||||||||||||||||||
Sbjct  31029  GCGACGCAAGCCTATGCCTTGTCGCGTGGTGTGGCCTATCTCAATGATATTCGCGGTTTT
31088

Query  60     CCAGACGCTGCGTTCTATCCGCAATTGGCGAAATCATCTGCCAAACTCGTCGTTATGCAT  119
              ||||||||||||||||||||||||||||||||||||||||||||||||||||||||||||
Sbjct  31089  CCAGACGCTGCGTTCTATCCGCAATTGGCGAAATCATCTGCCAAACTCGTCGTTATGCAT
31148

Query  120    TCGGTGCAAGACGGGCAGGCAGATCGGCGCGAGGCACCCGCTGGCGACATCATGGATCAC
179
              ||||||||||||||||||||||||||||||||||||||||||||||||||||||||||||
Sbjct  31149  TCGGTGCAAGACGGGCAGGCAGATCGGCGCGAGGCACCCGCTGGCGACATCATGGATCAC
31208

Query  180    ATTGCGGCGTTCTTTGACGCGCGCATCGCGGCGCTGACGGGTGCCGGTATCAAACGCAA  238
              ||||||||||||||||||||||||||||||||||||||||||||||||||||||||||||
Sbjct  31209  ATTGCGGCGTTCTTTGACGCGCGCATCGCGGCGCTGACGGGTGCCGGTATCAAACGCAA
31267
```

Figure 5: Snapshot of the gene SULII gene sequence alignment.

Table 2
The results of the QnrB sequence alignment and phenotypic.

Isolate	Substitution Count	Resistance (CIP)	MDR	Biofilm Intensity
1	8	R	Yes	Moderate
2	8	R	NO	Moderate
3	8	S	NO	Moderate

Table 3
Summary of the gene SULII sequence alignment results.

***Klebsiella pneumoniae* SULII**						
S.N.	**Type of substitution**	**Location**	**Nucleotide**	**Sequence ID with compare**	**Source**	**Identities**
1	GAP	31037	-/A	CP153458.1	*Klebsiella pneumoniae* strain NK_H2_020 plasmid pNK_H2_020.1, complete sequence	**99%**
2	TRANSVERSION TRANSVERSION	541230 541232	A/T C/G	CP064549.1	*Klebsiella pneumoniae* strain 2024CK-00847 chromosome, complete genome	**99%**
3	GAP GAP	85373 85377	-/C A/-	OQ821095.1	*Klebsiella pneumoniae* strain 11A19CPO086 plasm p11A19086_A_KPC, complete sequence	**99%**

Figure 6: Snapshot of the gene SULL gene sequence alignment.

Table 4
The results of the SULII sequence alignment and phenotypic.

Isolate	Substitution Count	Resistance (SXT)	MDR	Biofilm Intensity
1	1 (low)	R	Yes	Moderate
2	2 (moderate)	S	No	Moderate
3	2 (moderate)	S	No	Moderate

Table 5
Summary of the gene SULL sequence alignment results.

S.N.	Type of substitution	Location	Nucleotide	Sequence ID with compare	Source	Identities
1	Transition	93481	C/T	CP110179.1	*Klebsiella pneumoniae* strain XYJ-CZA-R plasmid pXYJ-CZA-R-2, complete sequence	98.75%
	GAP	93489	-/C			
	GAP	93471	-/C			
	Transversion	93873	G/C			
	Transversion	93874	C/G			
2	GAP	93489	-/C	CP110179.1	*Klebsiella pneumoniae* strain XYJ-CZA-R plasmid pXYJ-CZA-R-2, complete sequence	99.25%
	Transversion	93872	C/A			
3	Transversion	303	C/A	OW968456.1	*Klebsiella pneumoniae* isolate 1961 genome assembly, plasmid: P3	99.24%
	Transversion	304	G/C			
	Transversion	305	C/G			

Table 6
The results of the SULL sequence alignment and phenotypic.

Isolate	Substitution Count	Resistance (SXT)	MDR	Biofilm Intensity
1	5	R	Yes	Moderate
2	2	S	No	Moderate
3	3	S	No	Moderate

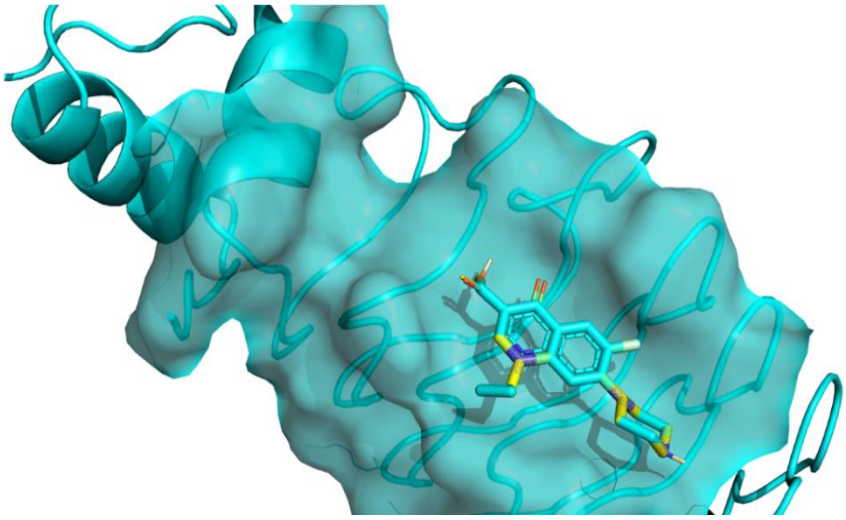

Figure 7: Focused docking places ciprofloxacin in a shallow surface groove on QnrB1.

This resulted in a tight cluster of alternatives within ~3.6–6.8 Å RMSD (modes 3–5, 7–9), suggesting a reproducible binding region. Two focused poses showed very large RMSD values (~55–59 Å), indicating remote, low-probability placements relative to the main cluster. Overall, focusing on the search produced ~0.9 kcal/mol better top affinity and clearer pose convergence than blind docking. Figure 7 shows focused docking of ciprofloxacin onto QnrB1 (PDB 2XTY), which converged on a solvent-exposed groove on the PRP surface, adjacent to the flexible resistance loops.

In the best pose (Table 7; −6.08 kcal/mol), the quinolone ring lies parallel to the local surface. The polar groups orient toward the rim of the pocket, consistent with weak-to-moderate, surface-mediated contacts rather than a buried active-site interaction.

As depicted in figure 8, the top-focused pose summarizes the important interactions between ligand and protein. The first pose in table 7, with an energy of −6.08 kcal/mol, forms a small network of polar contacts at the rim of a shallow surface groove on QnrB1 (chain A). In the 2D map, ciprofloxacin engages Asn139 and Asn118 by conventional H-bonds, with additional weak C–H···O contacts to Glu138/Glu160. The C6-fluorine shows a halogen contact toward Asn139, while Gly158–Gly159, Ser179 and Glu180 contribute Van-der-Waals stabilization. This pattern anchors the planar quinolone along the pocket edge rather than in a buried catalytic site.

Table 7
Blind vs. focused docking of ciprofloxacin to QnrB1 (PDB: 2XTY) using Auto Dock Vina.

Docking type	Mode	Affinity (kcal/mol)	RMSD lower bound (Å)	RMSD upper bound (Å)
Blind	1	–5.173	0	0
	2	–5.093	1.764	2.435
	3	–4.738	3.726	7.443
	4	–4.731	3.4	6.719
	5	–4.712	5.77	8.365
	6	–4.589	2.551	4.183
	7	–4.585	3.692	5.84
	8	–4.555	3.722	6.324
	9	–4.362	1.984	3.424
Focused	1	–6.080	0	0
	2	–6.002	54.89	58.88
	3	–5.942	3.58	6.17
	4	–5.838	3.699	5.917
	5	–5.818	6.399	10.5
	6	–5.801	53.42	57.21
	7	–5.749	5.433	8.505
	8	–5.727	3.8	6.388
	9	–5.664	6.775	9.667

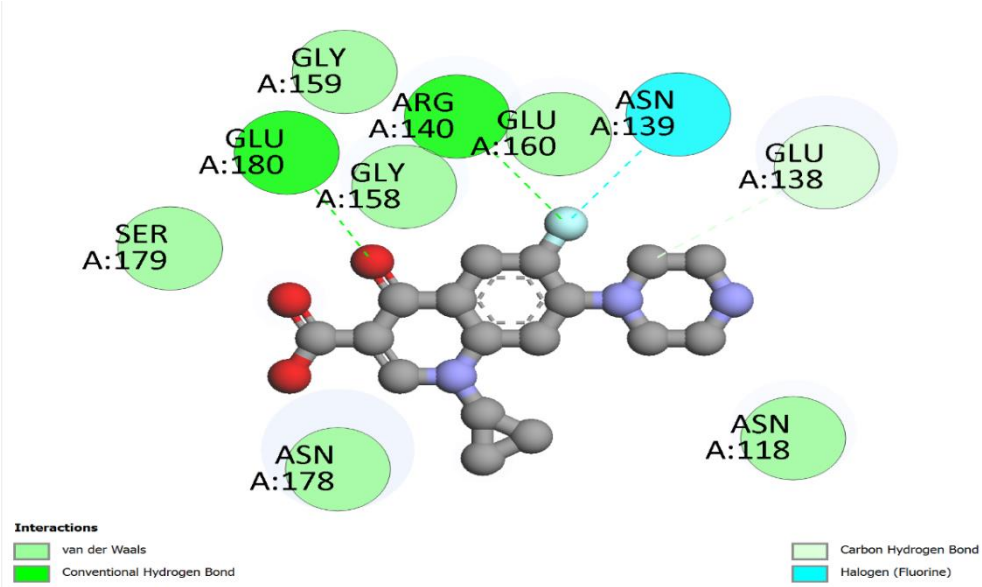

Figure 8: 2D interaction map of the focused docking pose of ciprofloxacin on QnrB1.

For each run, the top nine poses are listed with predicted binding free energy (Affinity, kcal/mol) and RMSD to the top-ranked pose (lower/upper bound, Å). Blind docking sampled the entire protein surface; focused docking restricted the search to the putative groove identified during inspection of the blind poses. Poses with very large RMSD values (>50 Å) represent distant, alternative sites and were treated as decoys.

Discussion

The current study proposes compelling evidence for a robust relationship among biofilm formation and multidrug-resistant (MDR) phenotypes in clinical isolates of *K. pneumoniae*. Particularly, all isolates showed biofilm-producing capability, with a substantial quantity-demonstrating moderate to strong biofilm formation. This surveillance supports with the well-recognized role of *K. pneumoniae* as a major opportunistic pathogen in healthcare sites[34]. Our data expose a clear association among the intensity of biofilm formation and resistance range across multiple antibiotic classes, comprising of carbapenems and third, fourth-generation cephalosporin. This underlines the clinical consequence of biofilm-mediated protection, as biofilms serve as a physical barrier that obstructs antibiotic penetration and donates to the perseverance of chronic and recurrent infections[2]. Isolates presenting robust biofilm formation also showed raised resistance levels, proposing a synergistic interaction among phenotypic and genotypic

resistance mechanisms[6]. The identical, high-level biofilm production perceived here offers a plausible mechanistic explanation for the MDR phenotypes documented. Besides, the heatmap analysis visually strengthens the co-occurrence of strong biofilm formation with MDR, constant with the 100% MDR occurrence detected in this group.

Genetically, the universal existence of plasmid-mediated quinolone resistance (PMQR) gene QnrB in our isolates, beside recurrent ciprofloxacin non-susceptibility, proposes a mechanistic supporting for this component of the MDR phenotype. All isolates accepted QnrB and showed multidrug resistance with dominant ciprofloxacin non-susceptibility (Table 1), though variants in quinolone susceptibility perform to comprise added determinants beyond QnrB polymorphisms. Structural modeling through molecular docking delivered insight into the mechanism of QnrB1, exposing ciprofloxacin binding to a shallow, solvent-exposed groove relatively than a canonical active site.

This interface is distinctive of Qnr proteins that transiently shield DNA gyrase from fluoroquinolones, thereby elevating MIC values and contributing to resistance[9]. Minor QnrB sequence variants and the lack of a direct association with ciprofloxacin resistance propose that high-level quinolone resistance naturally rises from a combination of PMQR genes, chromosomal mutations within quinolone resistance-determining regions (QRDRs e.g. gyrA, parC) and efflux pump overexpression[19].

Likewise, the high prevalence and conservation of the sulfonamide resistance genes SULII and SULL elucidate the frequent trimethoprim/sulfamethoxazole (SXT) resistance detected in our isolates. Together with the antibiograms, the near-uniform existence of SULII propositions a genetic explanation for recurrent trimethoprim/sulfamethoxazole non-susceptibility saw in this collection. If desirable, we can translate aligned segment to amino acids to description whether any substitutions are synonymous or non-synonymous within encoded region. This pattern proposes that SXT resistance is not explained by minor SULII sequence variant within the amplicon alone (Table 4). Other factors, for instance gene dosage or expression, probable contribute to the resistance.

Likewise, the alterations in trimethoprim–sulfamethoxazole response possible reflect factors elsewhere minor SULL polymorphisms. Thus, the substitution burden in SULL does not map directly to SXT phenotype or MDR status. SXT response likely depends on numerous factors. The localization of these genes on mobile genetic elements such as plasmids, eases their horizontal transfer and extent within bacterial populations[14]. Nevertheless, data have exposed a gap among subtle variants in the sequence of these genes and pattern of SXT resistance[24]. This outcome strongly advises that SXT resistance is not entirely dependent on a simple gene sequence but is a multifactorial phenomenon. Causal factors may comprise differences in gene expression, gene dosage (i.e. plasmid copy number), or presence of other factors that determine resistance. Examples of these factors are sul1 or dfrA variants that cause trimethoprim resistance[32]. These genes are frequently positioned in mobile elements, allowing co-selection and rapid evolution of resistance[27]. The significant differences between genotype and phenotype for both quinolone and SXT resistance highpoint the complexity of resistance mechanisms. They also demonstrate the restrictions of relying on the discovery of a single gene or its simple polymorphisms to guess clinical consequences.

Consequently, the experimental verdicts are supported by preceding studies and authorize that *K. pneumoniae* resistance is a network trait. This resistance outcome from a structural-regulatory-gene synergy. Hence, accrediting it to a local polymorphism in QnrB, or SULII/SULL, makes explanatory power absent unless maintained by measurements of dosage, expression context, biofilm status and mechanisms of excretion and permeability.

Our study deals with mutual numerous methods, comprising of CLSI-based AST characterization, gene confirmation and sequencing and biofilm quantification. We also further a structural-computational dimension with the inference of need for WGS/qPCR/transcriptomics. This style places our study within the most current trajectory of the field and donates to bridging a recurring gap between “gene” and “phenomenon”. Our work also establishes practical follow-up programs that can be tested on larger and more diverse sets of clinical isolates. In our view, collecting convincing indication of interconnection in this field requires three complementary approaches:

1. Whole-genome sequencing to identify plasmid copy number, gene promoters, insertion sites and load of additional determinants (e.g. sul1/sul3 and dfrA).
2. Transcriptomic profiling in suspension and biofilm states to measure regulatory transitions and excretion/ permeability dynamics.
3. Advanced structural models (e.g. long-time molecular dynamics) to track behavior of the pharmacological restrictor on the QnrB1 surface and directly relate it to *in vitro* markers such as MIC and MBC.

Conclusion

This study offers compelling indication that *K. pneumoniae* exhibits antibiotic resistance through a multifactorial network, rather than a single-gene mechanism. Our findings highpoint the interaction of regulatory, structural and efflux-mediated pathways, beside new-identified determinants for instance QnrB, SULII and SULL in varied clinical isolates. Integrating phenotypic and genotypic analyses comprising of AST according to CLSI, PCR/Sanger sequencing, quantitative chemical development valuation and structural computational modeling permit us to define what may be termed an initial “protection threshold,” that consequently

develops into a robust resistance phenotype through synergistic influences of altered permeability, overexpressed efflux pumps and potential QRDR mutations.

The data exposes a strong association among biofilm severity and expanded multidrug resistance (MDR) profiles. Minor sequence variations in QnrB/SULII/SULL paralleled with assessable differences in susceptibility, highlighting the complex, networked nature of resistance and interesting reductionist single-gene interpretations. Structural modeling of QnrB1 provides mechanistic perception, signifying its role in diminishing fluoroquinolone binding though, maximal clinical resistance involves the contribution of extra chromosomal and regulatory elements.

From a translational perception, these results underline the necessity of moving for mere detection of resistance genes to a comprehensive assessment of their expression, structural context and functional influence. We suggest an integrated workflow including:
1. WGS to map genetic architecture, insertion sites, plasmid copy number and auxiliary markers (for instances QRDR, dfrA/sul1/sul3 mutants).
2. Transcriptomic profiling under condition of planktonic and biofilm to evaluate dynamic changes in gene expression and efflux/permeability mechanisms.
3. Use quantitative PCR to regulate plasmid-borne gene dosage.
4. Functional assays assessing drug efflux and permeability together with standard AST.

Combining these methodologies into a combined diagnostic pathway can improve genotype-to-phenotype prediction, allowing more detailed and individualized therapeutic strategies. Particularly, agents for instance tigecycline and colistin reserved relative effectiveness in our isolates, deserving further investigation in larger partners. We concede limitations comprising the localized and moderately small sample size and the lack of direct measurements of gene dosage, expression and efflux activity. However, this study binds multiple layers of indication from phenotypic remark to structural modeling supportive the current view of resistance as a unified network rather than a single-gene phenomenon.

In conclusion, we promote for sustained research integrating WGS, transcriptomics and functional biofilm studies. Such programs hold potential for emerging anti-biofilm and efflux-targeted therapeutic strategies, attractive of the efficacy of conventional antimicrobials and eventually qualifying the clinical influence of MDR *K. pneumoniae*. This work sets a robust basis for evidence-based therapeutic strategies and innovative interventions against a pathogen of important clinical concern.

References

1. Abdelrahim S.S., Hassuna N.A., Waly N.G., Kotb D.N., Abdelhamid H. and Zaki S., Coexistence of plasmid-mediated quinolone resistance (PMQR) and extended-spectrum beta-lactamase (ESBL) genes among clinical Pseudomonas aeruginosa isolates in Egypt, *BMC Microbiology*, **24(1)**, 175, doi: https://doi.org/10.1186/s12866-024-03319-z **(2024)**

2. Abebe G.M., The role of bacterial biofilm in antibiotic resistance and food contamination, *International Journal of Microbiology*, **2020(1)**, 1705814, doi: https://doi.org/10.1155/2020/1705814 **(2020)**

3. Almatroudi A., Biofilm resilience: Molecular mechanisms driving antibiotic resistance in clinical contexts, *Biology*, **14(2)**, 165, doi: https://doi.org/10.3390/biology14020165 **(2025)**

4. Amel R. et al, Molecular mechanisms impact on fluoroquinolone resistance among E. coli from enteric carriage monitoring before prostate biopsy and earliest description of qnr B81, *Scientific Reports*, **14(1)**, 29324, doi: https://doi.org/10.1038/s41598-024-77844-2 **(2024)**

5. Araújo D. et al, Emerging approaches for mitigating biofilm-formation-associated infections in farm, wild and companion animals, *Pathogens*, **13(4)**, 320, doi: https://doi.org/10.3390/pathogens13040320 **(2024)**

6. Behzadi P. et al, Relationship between biofilm-formation, phenotypic virulence factors and antibiotic resistance in environmental *Pseudomonas aeruginosa*, *Pathogens*, **11(9)**, 1015, doi: https://doi.org/10.1016/j.micpath.2021.104922 **(2022)**

7. Ceballos-Garzon A., Holzapfel M., Welsch J. and Mercer D., Identification and antifungal susceptibility patterns of reference yeast strains to novel and conventional agents: a comparative study using CLSI, EUCAST and Sensititre YeastOne methods, *JAC-Antimicrobial Resistance*, **7(2)**, dlaf040, doi: https://doi.org/10.1093/jacamr/dlaf040 **(2025)**

8. Coenye T., Bové M. and Bjarnsholt T., Biofilm antimicrobial susceptibility through an experimental evolutionary lens, *NPJ Biofilms and Microbiomes*, **8(1)**, 82, doi: https://doi.org/10.1038/s41522-022-00346-4 **(2022)**

9. Dhara L. and Tripathi A., Role of gyrase A/B double mutations along with Qnr genes in development of higher ciprofloxacin resistance among Pathogenic *Escherichia coli* and *Klebsiella pneumoniae*, *Microbial Pathogenesis*, 107946, doi: https://doi.org/10.1016/j.micpath.2025.107946 **(2025)**

10. Doyle R.M. et al, Discordant bioinformatic predictions of antimicrobial resistance from whole-genome sequencing data of bacterial isolates: an inter-laboratory study, *Microbial Genomics*, **6(2)**, e000335, doi: https://doi.org/10.1099/mgen.0.000335 **(2020)**

11. Goswami Uttaron and Medhi Nayan, Scope of Implementation of Low Salinity Nanofluid to Improve Oil Recovery in a Part of the Hapjan Oil Field of Upper Assam Basin, *Res. J. Chem. Environ.*, **28(2)**, 100-109 **(2024)**

12. He Y.Z. et al, Novel plasmid-borne fimbriae-associated gene cluster participates in biofilm formation in *Escherichia coli*, *Microbial Drug Resistance*, **27(12)**, 1624-1632 **(2021)**

13. Hii S.Y.F. et al, Antibiotic susceptibility of clinical Burkholderia pseudomallei isolates in northeast Thailand from

2015 to 2018 and the genomic characterization of β-lactam-resistant isolates, *Antimicrobial Agents and Chemotherapy*, **65(5)**, doi: https://doi.org/ 10.1128/aac.02230-20 **(2021)**

14. Horne T., Orr V.T. and Hall J.P., How do interactions between mobile genetic elements affect horizontal gene transfer?, *Current Opinion in Microbiology*, **73**, 102282, doi: https://doi.org/10.1016/j.mib.2023.102282 **(2023)**

15. Hussein R.A., Al-Kubaisy S.H. and Al-Ouqaili M.T., The influence of efflux pump, outer membrane permeability and β-lactamase production on the resistance profile of multi, extensively and pandrug resistant *Klebsiella pneumoniae*, *Journal of Infection and Public Health*, **17(11)**, 102544, doi: https://doi.org/10.1016/j.jiph.2024.102544 **(2024)**

16. Hu Y., Anes J., Devineau S. and Fanning S., *Klebsiella pneumoniae*: prevalence, reservoirs, antimicrobial resistance, pathogenicity and infection: a hitherto unrecognized zoonotic bacterium, *Foodborne Pathogens and Disease*, **18(2)**, 63-84, doi: https://doi.org/10.1089/fpd.2020.2847 **(2021)**

17. Igere B., Onohuean H. and Nwodo U., Modern knowledge-scape possess petite influence on the factual persistence of resistance determinants (ARGs/MGEs): a map and assessment of discharged wastewater and water bodies, *Heliyon*, **8(12)**, doi: https://doi.org/10.1016/j.heliyon.2022.e12253 **(2022)**

18. Juraschek K. et al, Characterization of qnrB-carrying plasmids from ESBL-and non-ESBL-producing *Escherichia coli*, *BMC Genomics*, **23(1)**, 365, doi: https://doi.org/10.1186/s12864-022-08564-y **(2022)**

19. Kareem S.M. et al, Detection of gyrA and parC mutations and prevalence of plasmid-mediated quinolone resistance genes in *Klebsiella pneumoniae*, *Infection and Drug Resistance*, 555-563, doi: https://doi.org/10.2147/IDR.S275852 **(2021)**

20. Karygianni L., Ren Z., Koo H. and Thurnheer T., Biofilm matrixome: extracellular components in structured microbial communities, *Trends in Microbiology*, **28(8)**, 668-681, doi: https://doi.org/10.1016/j.tim.2020.03.016 **(2020)**

21. Kashefieh M., Hosainzadegan H., Baghbanijavid S. and Ghotaslou R., The molecular epidemiology of resistance to antibiotics among *Klebsiella pneumoniae* isolates in Azerbaijan, Iran, *Journal of Tropical Medicine*, **2021(1)**, 9195184, doi: https://doi.org/10.1155/2021/9195184 **(2021)**

22. Kirti N., Krishna S.S. and Shukla D., Salmonella infections: an update, detection and control strategies, In Salmonella-Current Trends and Perspectives in Detection and Control, IntechOpen, doi: https://doi.org/10.5772/intechopen.1004835 **(2024)**

23. La Rosa G. et al, Rapid screening for SARS-CoV-2 variants of concern in clinical and environmental samples using nested RT-PCR assays targeting key mutations of the spike protein, *Water Research*, **197**, 117104, doi: https://doi.org/10.1016/j.watres.2021.117104 **(2021)**

24. Lima T., Domingues S. and Da Silva G.J., Manure as a potential hotspot for antibiotic resistance dissemination by horizontal gene transfer events, *Veterinary Sciences*, **7(3)**, 110, doi: https://doi.org/10.3390/vetsci7030110 **(2020)**

25. Liu P., Liu J. and Xiao L., A unified pansharpening method with structure tensor driven spatial consistency and deep plug-and-play priors, *IEEE Transactions on Geoscience and Remote Sensing*, **60**, 1-14, doi: https://doi.org/10.1109/TGRS.2022.3225563 **(2022)**

26. Li Y., Kumar S. and Zhang L., Mechanisms of antibiotic resistance and developments in therapeutic strategies to combat *Klebsiella pneumoniae* infection, *Infection and Drug Resistance*, 1107-1119, doi: https://doi.org/10.2147/IDR.S453025 **(2024)**

27. Mazhar S.H. et al, Co-selection of antibiotic resistance genes and mobile genetic elements in the presence of heavy metals in poultry farm environments, *Science of The Total Environment*, **755**, 142702, doi: https://doi.org/10.1016/j.scitotenv.2020.142702 **(2021)**

28. Michaelis C. and Grohmann E., Horizontal gene transfer of antibiotic resistance genes in biofilms, *Antibiotics*, **12(2)**, 328, doi: https://doi.org/10.3390/antibiotics12020328 **(2023)**

29. Müller C.Z., Resistance profile and genetic features associated with plasmid-mediated quinolone resistance in *Escherichia coli* isolates from wastewater and clinical samples, doi: http://hdl.handle.net/10183/289172 **(2024)**

30. Peng C., Yao M., Liu J., Zhang Q., Yuan G. and Ma Q., The relationship between integrons, antibiotic resistance genes and SXT resistance in Shigella flexneri strains, *American Journal of Translational Research*, **16(5)**, 1925, doi: https://doi.org/10.62347/SNRQ6766 **(2024)**

31. Peters U., Sherling H.R. and Chin-Yee B., Hasty generalizations and generics in medical research: A systematic review, *Plos One*, **19(7)**, e0306749, doi: https://doi.org/10.1371/journal.pone.0306749 **(2024)**

32. Poey M.E., De Los Santos E., Aznarez D., García-Laviña C.X. and Laviña M., Genetics of resistance to trimethoprim in cotrimoxazole resistant uropathogenic Escherichia coli: integrons, transposons and single gene cassettes, *Frontiers in Microbiology*, **15**, 1395953, doi: https://doi.org/10.3389/fmicb.2024.1395953 **(2024)**

33. Sharma S., Mohler J., Mahajan S.D., Schwartz S.A., Bruggemann L. and Aalinkeel R., Microbial biofilm: a review on formation, infection, antibiotic resistance, control measures and innovative treatment, *Microorganisms*, **11(6)**, 1614, doi: https://doi.org/10.3390/MICROORGANISMS11061614 **(2023)**

34. Stec J. et al, Opportunistic pathogens of recreational waters with emphasis on antimicrobial resistance—a possible subject of human health concern, *International Journal of Environmental Research and Public Health*, **19(12)**, 7308, doi: https://doi.org/10.3390/ijerph19127308 **(2022)**

35. Tuytschaever T., Raes K. and Sampers I., Biofilm detection in the food industry: Challenges in identifying biofilm eps markers and analytical techniques with insights for Listeria monocytogenes, *International Journal of Food Microbiology*, 111091 **(2025)**

36. Uruén C., Chopo-Escuin G., Tommassen J., Mainar-Jaime R.C. and Arenas J., Biofilms as promoters of bacterial antibiotic

resistance and tolerance, *Antibiotics*, **10(1)**, 3, doi: https://doi.org/10.3390/ANTIBIOTICS10010003 **(2020)**

37. Wang G., Zhao G., Chao X., Xie L. and Wang H., The characteristic of virulence, biofilm and antibiotic resistance of Klebsiella pneumoniae, *International Journal of Environmental Research and Public Health*, **17(17)**, 6278, doi: https://doi.org/10.3390/ijerph17176278 **(2020)**

38. Yaseen M., Genetic and in-silico approaches for investigating the mechanisms of ciprofloxacin resistance in *Salmonella typhi*: Mutations, extrusion and antimicrobial resistance, doi: https://doi.org/10.1016/j.heliyon.2024.e38333 **(2024)**.

(Received 29th September 2025, accepted 30th Ocrober 2025)